Integral Sliding Mode Control and Gain-Scheduled Modified Utkin Observer for an Underground Coal Gasification Energy Conversion Process

Ali Arshad Uppal[1], Saif Siddique Butt[2], Aamer Iqbal Bhatti[3] and Harald Aschemann[4]

***Abstract*— One of the challenging control problems of an underground coal gasification (UCG) process involves maintaining a desired heating value from the extracted product gases. In this paper, a model-based control and state estimation of UCG process is described. For the purpose of control and state estimation, a sophisticated model of UCG process, based on partial differential equations is approximated with a gain-scheduled nonlinear control-oriented model. Based on this approximated plant model, a robust integral sliding mode control is designed to track a desired heating value. Furthermore, for the estimation of unknown states of the system, a gain-scheduled modified Utkin observer is designed as well. The robustness of the nonlinear control and estimation techniques is exploited by introducing parametric uncertainties in the UCG plant. The simulation results highlight the effectiveness of the proposed nonlinear control and estimation techniques in comparison to a conventional PI controller.**

I. INTRODUCTION

Due to the stringent environmental legislations on clean energy production by means of coal, measures have been taken for employing underground coal gasification process (UCG) in some parts of the world [1], [2]. Gasification is one of the clean coal technologies which involves the conversion of coal beds beneath the surface of the earth into useful synthesis gas (syngas). For this purpose, two wells are drilled from surface to the coal seam and a permeable link is established between the wells. Afterwards, oxidants (air and steam (H_2O), or (O_2) and H_2O or only air) are injected from one well which chemically react with already ignited coal to produce syngas.

Most of the industrial applications, e.g., integrated gasification combined cycle turbines (IGCC), require a desired heating value of the syngas [3]. In practice, the composition and flow rate of injected oxidants act as manipulated variables to control the heating value in a UCG plant. The presence of parametric uncertainties, modeling inaccuracies as well as unknown disturbances acting on the system impose a challenging control problem.

In [4] and [5], a conventional PID controller is designed for a lab scale UCG setup to control concentration, temperature and heating value of product gases. Moreover, a sliding mode control (SMC) and super-twisting control are developed for a simplified time domain model of UCG in [6], [7], [8]. However, all the system's states are assumed to be measurable in [6], which is usually not the case. The work in [7], [8] employs a simplified model of the UCG process to compute estimates for controller gains. Due to the physical structure of a UCG plant, it is not possible to measure steam concentration, solid temperature and densities of coal and char. In this paper, an integral sliding mode is proposed to track desired heating value for the control-oriented model of UCG plant under the influence of parametric uncertainties as well as measurement noise. Furthermore, unknown states of the system are reconstructed using a gain-scheduled modified Utkin observer [9], [10].

This paper is arranged as follows: In Section II, the nonlinear control-oriented model of the UCG plant is presented. The integral SMC and the gain-scheduled modified Utkin observer for the UCG plant are designed in Sections III and IV, respectively. The control implementation is discussed in Section V. The simulation results of the proposed and a conventional PI controller are described in Section VI. Finally, the paper is concluded in Section VII.

II. UCG PROCESS MODEL

The nonlinear control-oriented model of UCG process [6] presented in this section, is derived from one-dimensional packed models of [11] and [12]. The mathematical model comprises of mass and energy balances of solids and gases. The dynamics of coal density ρ_{coal} (g/cm^3), char density ρ_{char} (g/cm^3) and solid temperature T_s (K) are given by

$$\begin{aligned}\dot{\rho}_{\mathrm{coal}} &= -M_1 R_1 \ , \\ \dot{\rho}_{\mathrm{char}} &= -M_2(a_{s_{2,1}} R_1 - R_2 - R_3), \\ \dot{T}_s &= \frac{1}{C_s}\big(h_t(T - T_s) - \Delta q_2 R_2 - \Delta q_3 R_3\big) \ . \end{aligned} \tag{1}$$

Applying mass balance on the gases (CO, CO_2, H_2, CH_4, H_2O, O_2, N_2, Tar) results in time-derivatives of gases concentration C_i (mol/cm^3) given as follows

$$\begin{aligned}\dot{C}_{\mathrm{CO}} &= a_{1,1} R_1 + R_3 - \beta C_{\mathrm{CO}} \ , \\ \dot{C}_{\mathrm{CO_2}} &= a_{2,1} R_1 + R_2 - \beta C_{\mathrm{CO_2}} \ , \\ \dot{C}_{\mathrm{H_2}} &= a_{3,1} R_1 + R_3 - \beta C_{\mathrm{H_2}} \ , \\ \dot{C}_{\mathrm{CH_4}} &= a_{4,1} R_1 - \beta C_{\mathrm{CH_4}} \ , \\ \dot{C}_{\mathrm{Tar}} &= a_{5,1} R_1 - \beta C_{\mathrm{Tar}} \ , \end{aligned} \tag{2}$$

[1]Ali A. Uppal is with the Department of Electrical Engineering, COMSATS Institute of Information Technology, Islamabad, Pakistan ali_arshad@comsats.edu.pk

[2]Saif S. Butt is with the IAV Development GmbH, Gifhorn, Germany saif.siddique.butt@iav.de

[3]Aamer I. Bhatti is with the Department of Electrical Engineering, Capital University of Science and Technology, Islamabad, Pakistan aib@cust.edu.pk

[4]H. Aschemann is with Chair of Mechatronics, University of Rostock, Rostock, Germany harald.aschemann@uni-rostock.de

$$\dot{C}_{\mathrm{H_2O}} = a_{6,1}R_1 + a_{6,2}R_2 + a_{6,3}R_3 - \beta C_{\mathrm{H_2O}} + \frac{\alpha}{L}u \ ,$$
$$\dot{C}_{\mathrm{O_2}} = a_{7,2}R_2 - \beta C_{\mathrm{O_2}} + \frac{\delta}{L}u \ ,$$
$$\dot{C}_{\mathrm{N_2}} = -\beta C_{\mathrm{N_2}} + \frac{\gamma}{L}u \ . \tag{3}$$

Herein, R_1, R_2 and R_3 are the reaction rates which are a function of the gases concentrations, solid temperature as well as densities of coal and char, respectively. The empirical relationships of these reaction rates are as follows:

$$R_1 = 5\frac{\rho_{\mathrm{coal}}}{M_1}\exp\left(\frac{-6039}{T_s}\right), R_{m_2} = \frac{1}{10}h_t m_{\mathrm{O_2}},$$
$$R_{c_2} = \frac{1}{M_2}\left(9.55\times10^8 \rho_{\mathrm{char}} m_{\mathrm{O_2}} P \exp\left(\frac{-22142}{T_s}\right)T_s^{-0.5}\right) ,$$
$$R_2 = \frac{1}{\frac{1}{R_{c_2}} + \frac{1}{R_{m_2}}} \ , R_{m_3} = \frac{1}{10}h_t m_{\mathrm{H_2O}}$$
$$R_{c_3} = \frac{\rho_2 m_{\mathrm{H_2O}}^2 P^2 \exp\left(5.052 - \frac{12908}{T_s}\right)}{M_2\left(m_{\mathrm{H_2O}}P + \exp\left(-22.216 + \frac{24880}{T_s}\right)\right)^2},$$
$$R_3 = \frac{1}{\frac{1}{R_{c_3}} + \frac{1}{R_{m_3}}} \ , \tag{4}$$

where $m_{\mathrm{O_2}}$ and $m_{\mathrm{H_2O}}$ are internal molar fractions of O_2 and H_2O. Mathematically, the molar fractions are expressed as

$$m_{\mathrm{O_2}} = \frac{C_{\mathrm{O_2}}}{C_T + C_{\mathrm{H_2O}}}, \ m_{\mathrm{H_2O}} = \frac{C_{\mathrm{H_2O}}}{C_T + C_{\mathrm{H_2O}}},$$
$$C_T = C_{\mathrm{CO}} + C_{\mathrm{CO_2}} + C_{\mathrm{H_2}} + C_{\mathrm{CH_4}} + C_{\mathrm{Tar}} + C_{\mathrm{O_2}} + C_{\mathrm{N_2}} \ .$$

The description of the model parameters is listed in Table. I. Furthermore, the nominal values of the parameter are reported in [6].

TABLE I: List of parameters and states.

Symbol	Description
M_i	Molecular weight (g/mol), $i = 1, 2$ for coal and char, respectively
T	Gas temperature (K)
$a_{s_{2,1}}$	Stoichiometric coefficient of char in coal pyrolysis reaction
h_t	Heat transfer coefficient (cal/s/K/cm^3)
C_s	Specific heat capacity of solids (cal/g/K)
R_i	Rate of a chemical reaction (mol/cm^3/s), $i = 1, 2, 3$ represents pyrolysis, char oxidation and steam gasification, respectively
$a_{i,j}$	Stoichiometric coefficient of gas i in reaction j
Δq_i	Heat of reaction i (cal/mol), $i = 1, 2$ represents char oxidation and steam gasification, respectively
L	Length of the reactor (cm)
βC_i	Approximation of spatial derivative (mol/cm^3/s) [6]
u	Flow rate of injected gases (moles/cm^2/s)
α, δ,γ	Percentages of H_2O, O_2 and N_2 in u

For the model-based control design, a control-oriented model is a prerequisite. The state vector $\boldsymbol{x}$ for the control-oriented model of UCG is chosen as

$$\boldsymbol{x} = [\rho_{\mathrm{coal}} \ \ \rho_{\mathrm{char}} \ \ T_s \ \ C_{\mathrm{CO}} \ \ C_{\mathrm{CO_2}} \ \ C_{\mathrm{H_2}} \ \ C_{\mathrm{CH_4}} \ \ C_{\mathrm{Tar}} \ \ C_{H_2O} \ \ C_{\mathrm{O_2}} \ \ C_{\mathrm{N_2}}]^T \ . \tag{5}$$

The data acquisition system for a UCG process employs a gas analyzer which measures the percentage volume content for dry gases. Nonetheless, this dried mixture of gases is deprived of steam (H_2O) [13], [7] and [14]. Therefore, the concentration of the gases can be directly determined from the volume content of each gas. Hence, the measurement vector $\boldsymbol{y_m}$ is given by

$$\boldsymbol{y_m} = \begin{bmatrix} C_{\mathrm{CO}} & C_{\mathrm{CO_2}} & C_{\mathrm{H_2}} & C_{\mathrm{CH_4}} & C_{\mathrm{Tar}} & C_{\mathrm{O_2}} & C_{\mathrm{N_2}} \end{bmatrix}^T \ . \tag{6}$$

Mathematically, the nonlinear control-oriented model given in Eq. (1) and Eq. (3) can be represented in a control-affine form, i.e,

$$\dot{\boldsymbol{x}} = \boldsymbol{f}(\boldsymbol{x}) + \boldsymbol{g}(\boldsymbol{x})u \ . \tag{7}$$

In order to control heating value of a UCG process, an integral sliding mode control (ISMC) is described in the next section.

III. Integral sliding Mode Control Design

In this section, a tracking ISMC is designed for the heating value H_v of the UCG process. Mathematically, this heating value is computed as

$$H_v = H_{\mathrm{CO}}\chi_{\mathrm{CO}} + H_{\mathrm{H_2}}\chi_{\mathrm{H_2}} + H_{\mathrm{CH_4}}\chi_{\mathrm{CH_4}} \ , \tag{8}$$

where the mole fraction χ_i is given by

$$\chi_i = \frac{C_i}{C_T}.$$

Herein, H_i is the heat of combustion of gas i (KJ/mol). For the control purpose, an integral sliding surface σ is chosen as follows

$$\sigma = e + k_i\int_0^t e dt, \quad \text{and} \quad e = H_v - H_{v_r} \ , \tag{9}$$

where k_i and H_{v_r} are the integral gain and desired heating value, respectively. The design of the sliding variable ensures the exponential convergence of e during an ideal sliding motion, i.e., $\sigma = 0$. The dynamics of the system under sliding motion is governed by

$$\dot{\sigma} = 0 \implies \dot{e} + k_i e(t) = 0 \ . \tag{10}$$

Hence, choosing a strictly positive k_i leads to an exponential convergence in a finite-time. The control input which forces the system trajectory to the sliding manifold $\sigma = 0$ is given by

$$u = u_{eq} + \kappa\,\mathrm{sgn}(\sigma) \ , \tag{11}$$

where u_{eq} is the part of the control input which achieves $\dot{\sigma} = 0$, and $\kappa \in \mathbb{R}^+$ is a discontinuous gain which provides the required robustness against the modeling imperfections and external disturbances. The equivalent control input u_{eq}

derived from the nonlinear control-oriented model is given by

$$u_{eq} = \frac{L\big(C_{_T}(C_{_T}\phi + \theta + \beta) - \Omega - a_{_{R_1}}R_1 - a_{_{R_2}}R_2 - 2R_3\big)}{\delta + \gamma}, \tag{12}$$

where the intermediate terms in the control law are computed as follows

$$\begin{aligned}
\phi &= k_i e - \dot{H}_{v_r},\\
\Omega &= H_a C_{\mathrm{CO}} + H_b C_{\mathrm{H_2}} + H_c C_{\mathrm{CH_4}},\\
\theta &= R_1(H_a a_{1,1} + H_b a_{3,1} + H_c a_{5,1}) + R_3(H_a + H_b) - \beta\Omega,\\
a_{_{R_1}} &= a_{1,1} + a_{3,1} + a_{5,1},\\
a_{_{R_2}} &= 1 + a_{7,2}\ .
\end{aligned}$$

Proof: Finite-time convergence of sliding mode:

In order to prove the existence of a sliding mode, a positive definite Lyapunov functional is considered

$$V = \frac{1}{2}\sigma^T\sigma\ . \tag{13}$$

Taking time derivative of (13) and using the results of (9), (11) and (12)

$$\begin{aligned}
\dot{V} &= \sigma\dot{\sigma}\\
&= \sigma\big(-\kappa\,\mathrm{sgn}(\sigma) + f(t)\big)\\
&\leq -|\sigma|\big(\kappa - f_0\big),
\end{aligned} \tag{14}$$

where $||f(t)|| \leq f_o$ is a unknown but norm-bounded input disturbance or variation in the model parameters. If $\kappa > f_o + \tau$, where $\tau \in \mathbb{R}^+$, then

$$\dot{V} \leq -\tau|\sigma| \tag{15}$$

holds, and, hence, a finite-time convergence of sliding mode is guaranteed [15]. The control law (12) is a function of ρ_{coal}, ρ_{char}, T_s and $C_{\mathrm{H_2O}}$. As these states are not directly measurable, a gain-scheduled modified Utkin observer (GSMUO) is designed to estimate these unknown states.

IV. Gain-Scheduled Modified Utkin Observer

Using optimization techniques the nonlinear model according to (1) and (3) is approximated by a representation with a state-dependent system matrix, cf. [16]. The quasi-linear model of the UCG is given by

$$\begin{aligned}
\dot{\boldsymbol{x}} &= \boldsymbol{A}(\boldsymbol{x})\boldsymbol{x} + \boldsymbol{b}u,\\
\boldsymbol{y} &= \boldsymbol{C}\boldsymbol{x}\ ,
\end{aligned} \tag{16}$$

where $\boldsymbol{x} \in \mathbb{R}^{11}$, $\boldsymbol{A}(\boldsymbol{x}) \in \mathbb{R}^{11\times 11}$, $\boldsymbol{b} \in \mathbb{R}^{11}$ and $\boldsymbol{C} \in \mathbb{R}^{7\times 11}$. For the ease of derivation, the state-dependent part in the system matrix is not shown explicitly. In a conventional sliding mode observer, it is not trivial to choose switching gains to enforce sliding mode in finite time. To overcome this issue, a sliding mode observer extended with an additional Luenberger-type gain matrix, feeding back the output errors, is proposed to achieve a robust state re-construction [17]. Consider a possible coordinate transformation $\boldsymbol{x} \longrightarrow \boldsymbol{T}_c\boldsymbol{x}$, with

$$\boldsymbol{T}_c = \begin{bmatrix}\boldsymbol{N}_c^T & \boldsymbol{C}\end{bmatrix}^T, \tag{17}$$

where $\boldsymbol{N}_c \in \mathbb{R}^{4\times 7}$ spans the null space of $\boldsymbol{C}$. The linearized system in transformed coordinates is given by

$$\begin{bmatrix}\dot{\boldsymbol{z}}\\ \dot{\boldsymbol{y}}_m\end{bmatrix} = \boldsymbol{T}_c\boldsymbol{A}\boldsymbol{T}_c^{-1}\begin{bmatrix}\boldsymbol{z}\\ \boldsymbol{y}_m\end{bmatrix} + \boldsymbol{T}_c\boldsymbol{b}u\ . \tag{18}$$

According to new coordinates transformation, the unknown states are

$$\boldsymbol{z} = \begin{bmatrix}\rho_{\mathrm{coal}} & \rho_{\mathrm{char}} & T_s & C_{\mathrm{H_2O}}\end{bmatrix}^T. \tag{19}$$

The corresponding output matrix is

$$\boldsymbol{C}\boldsymbol{T}_c^{-1} = \begin{bmatrix}\boldsymbol{0}_{4\times 7} & \boldsymbol{I}_{7\times 7}\end{bmatrix}. \tag{20}$$

Now, the new system can be partitioned as follows

$$\boldsymbol{T}_c\,\boldsymbol{A}\,\boldsymbol{T}_c^{-1} = \left[\begin{array}{c:c}\boldsymbol{A}_{11} & \boldsymbol{A}_{12}\\ \hdashline \boldsymbol{A}_{21} & \boldsymbol{A}_{22}\end{array}\right]\ ,\ \text{and}\ \ \boldsymbol{T}_c\,\boldsymbol{B} = \left[\begin{array}{c}\boldsymbol{b}_1\\ \hdashline \boldsymbol{b}_2\end{array}\right]\ .$$

Rewriting the system dynamics leads to

$$\begin{aligned}
\dot{\boldsymbol{z}} &= \boldsymbol{A}_{11}\boldsymbol{z} + \boldsymbol{A}_{12}\boldsymbol{y}_m + \boldsymbol{b}_1 u\ ,\\
\dot{\boldsymbol{y}}_m &= \boldsymbol{A}_{21}\boldsymbol{z} + \boldsymbol{A}_{22}\boldsymbol{y}_m + \boldsymbol{b}_2 u\ .
\end{aligned} \tag{21}$$

The structure of the corresponding sliding mode observer is given by

$$\begin{aligned}
\dot{\hat{\boldsymbol{z}}} &= \boldsymbol{A}_{11}\hat{\boldsymbol{z}} + \boldsymbol{A}_{12}\hat{\boldsymbol{y}}_m + \boldsymbol{b}_1 u + \boldsymbol{L}\boldsymbol{\upsilon} - \boldsymbol{G}_1\boldsymbol{e}_y\,,\\
\dot{\hat{\boldsymbol{y}}}_m &= \boldsymbol{A}_{21}\hat{\boldsymbol{z}} + \boldsymbol{A}_{22}\hat{\boldsymbol{y}}_m + \boldsymbol{b}_2 u - \boldsymbol{\upsilon} - \boldsymbol{G}_2\boldsymbol{e}_y\,.
\end{aligned} \tag{22}$$

Here, $\hat{\boldsymbol{z}}$ and $\hat{\boldsymbol{y}}_m$ are the state estimates. $\boldsymbol{G}_1 \in \mathbb{R}^{4\times 7}$ and $\boldsymbol{G}_2 \in \mathbb{R}^{7\times 7}$ represent the Luenberger type gain matrices and yield the potential to provide robustness against certain class of uncertainties, furthermore $\boldsymbol{L} \in \mathbb{R}^{4\times 7}$ is a feedback gain matrix. The discontinuous vector $\boldsymbol{\upsilon}$ is defined by

$$\boldsymbol{\upsilon} = \begin{bmatrix} M_1\ \mathrm{sgn}(\hat{y}_{m,1} - y_{m,1})\\ M_2\ \mathrm{sgn}(\hat{y}_{m,2} - y_{m,2})\\ \vdots\\ M_7\ \mathrm{sgn}(\hat{y}_{m,7} - y_{m,7})\end{bmatrix}, \tag{23}$$

with $M_i \in \mathbb{R}^+$. The nonlinear switching terms guarantee finite-time convergence. By using (21) and (22), the error dynamics can be expressed as

$$\dot{\hat{\boldsymbol{e}}}_z = \boldsymbol{A}_{11}\hat{\boldsymbol{e}}_z + \boldsymbol{A}_{12}\hat{\boldsymbol{e}}_y + \boldsymbol{L}\boldsymbol{\upsilon} - \boldsymbol{G}_1\boldsymbol{e}_y\ , \tag{24}$$

$$\dot{\hat{\boldsymbol{e}}}_y = \boldsymbol{A}_{21}\hat{\boldsymbol{e}}_z + \boldsymbol{A}_{22}\hat{\boldsymbol{e}}_y - \boldsymbol{\upsilon} - \boldsymbol{G}_2\boldsymbol{e}_y\ . \tag{25}$$

where $\boldsymbol{e}_z = \hat{\boldsymbol{z}} - \boldsymbol{z}$ and $\boldsymbol{e}_y = \hat{\boldsymbol{y}}_m - \boldsymbol{y}_m$. Introducing a new error variable $\bar{\boldsymbol{e}}_z = \boldsymbol{e}_z + \boldsymbol{L}\,\boldsymbol{e}_y$, the resultant error dynamics with respect to the new state variables, $\bar{\boldsymbol{e}}_z$ and $\boldsymbol{e}_{y_m}$, can be expressed as

$$\left[\begin{array}{c}\dot{\bar{\boldsymbol{e}}}_z\\ \hdashline \dot{\boldsymbol{e}}_y\end{array}\right] = \left[\begin{array}{c:c}\bar{\boldsymbol{A}}_{11} & \bar{\boldsymbol{A}}_{12}\\ \hdashline \boldsymbol{A}_{21} & \bar{\boldsymbol{A}}_{22}\end{array}\right]\left[\begin{array}{c}\bar{\boldsymbol{e}}_z\\ \hdashline \boldsymbol{e}_y\end{array}\right] + \left[\begin{array}{c}\boldsymbol{0}\\ \hdashline -\boldsymbol{I}\end{array}\right]\boldsymbol{\upsilon}\,, \tag{26}$$

with the submatrices

$$\begin{aligned}\bar{\boldsymbol{A}}_{11} &= \boldsymbol{A}_{11} + \boldsymbol{L}\,\boldsymbol{A}_{21}\ ,\\ \bar{\boldsymbol{A}}_{12} &= \boldsymbol{A}_{12} - \bar{\boldsymbol{A}}_{11}\boldsymbol{L} - \boldsymbol{G}_1 + \boldsymbol{L}\,(\boldsymbol{A}_{22} - \boldsymbol{G}_2)\ ,\\ \bar{\boldsymbol{A}}_{22} &= \boldsymbol{A}_{22} - \boldsymbol{G}_2 - \boldsymbol{A}_{21}\,\boldsymbol{L}\ .\end{aligned} \tag{27}$$

According to (26), the state reconstruction problem has been transformed in to a regulation problem in $\boldsymbol{e}_y$ and $\bar{\boldsymbol{e}}_z$, with $\boldsymbol{v}$ as an auxiliary observer input.

Therefore, if $\boldsymbol{L}$ is designed in such a way that the matrix $\bar{\boldsymbol{A}}^*_{11}$ in (28) is Hurwitz, then the error $\boldsymbol{e}_z$ converges asymptotically

$$\boldsymbol{A}_{11} + \boldsymbol{L}\,\boldsymbol{A}_{21} = \bar{\boldsymbol{A}}^*_{11}\ , \tag{28}$$

similarly, $\boldsymbol{G}_2$ can be chosen to yield a stable design matrix $\bar{\boldsymbol{A}}^*_{22}$ in

$$\boldsymbol{A}_{22} - \boldsymbol{G}_2 - \boldsymbol{A}_{21}\,\boldsymbol{L} = \bar{\boldsymbol{A}}^*_{22}\ . \tag{29}$$

The matrices $\boldsymbol{L}$ and $\boldsymbol{G}_2$ are computed using LQR method which optimally places the eigenvalues of $\bar{\boldsymbol{A}}^*_{11}$ and $\bar{\boldsymbol{A}}^*_{22}$ in the complex left hand plane. Finally, $\boldsymbol{G}_1$ in (27) can be designed in such a way that $\bar{\boldsymbol{A}}_{12} = \boldsymbol{0}$ holds.

V. Control Implementation Scheme

Fig. 1 illustrates the overall implementation scheme of the ISMC in combination with a GSMUO. Nevertheless,

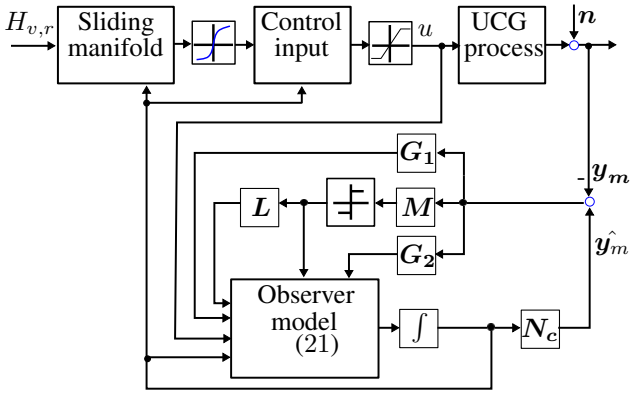

Fig. 1: Control implementation scheme for the UCG process.

a saturation block is included for the contol input to restrict negative flow rates. Furthermore, measurement noise $\boldsymbol{n}$ is introduced in the sensor measurements. Although the switching input $\boldsymbol{\sigma}$ in Eq. (11) offers the potential to provide robustness against certain classes of model uncertainty, it also introduces chattering, which is addressed by using the $\frac{\tanh}{\epsilon}$ function instead of the sgn function in the implementation. This results in a real sliding mode within a boundary layer ϵ instead of an ideal sliding mode. In short, a sliding mode is induced in the error associated with the output vector, whereas the error in the estimates of unknown states converges asymptotically.

VI. Simulation Results

In this section, a simulation analysis for the UCG plant along with the ISMC and GSMUO is described. In order to perform a thorough simulation analysis, the following points are considered in order to have real-time issues:

- An additive white Guassian noise with zero mean and variance of 0.02^2 is added in each concentration outputs C_i of the UCG plant. This variance corresponds to the typical measurement accuracy of gas analyzers used in the UCG process.
- In order to study the robustness property of the control and estimation strategies, parametric uncertainties of 2% are introduced in the nominal system parameters, namely P, β, h_t and C_s. It is worth mentioning that the integral sliding mode controller as well as the GSMUO contains the nominal system parameters.
- For the warm-up phase of the underground coal, it is necessary to burn the coal so that the gasification process can be successfully started. This situation is realized by operating the UCG plant in open-loop. For this purpose, the flow rate of the injected gases is kept at 2×10^{-4} moles/cm^2/s.
- The feedback control is activated after 20000s, when H_v reaches its maximum value.
- The GSMUO is in continuous operation during both the open-loop and closed-loop operations of UCG plant.

In order to study the estimation behavior of the observer, it is necessary to initialize both the UCG plant and observer with different initial conditions. The nonlinear control-oriented model of UCG process is initialized with the following states

$$\boldsymbol{x} = [0.5\ 0\ 497\ 0\ 0\ 0\ 0\ 0\ 0\ 4.2e{-}4\ 1.6e{-}3]^T. \tag{30}$$

On the other hand, the GSMUO is initialized with

$$\hat{\boldsymbol{x}} = [0.48\ 0\ 480\ 0\ 0\ 0\ 0\ 0\ 0\ 4.2e{-}4\ 1.6e{-}3]^T. \tag{31}$$

As mentioned in Section IV, the observer gain matrices $\boldsymbol{L}$ and $\boldsymbol{G}_2$ in (28) and (29) are designed using an LQR formulation. This, on the one hand, allows for specifying relative weights to the unknown states and measurements. On the other hand, an optimal gain can be obtained for the given operating conditions of the quasi-linear model of the UCG plant. For optimal $\boldsymbol{L}$, the weighting matrices $\boldsymbol{Q}$ and $\boldsymbol{R}$ representing the weights for $\boldsymbol{e_z}$ and $\boldsymbol{e_y}$ in the LQR cost function are chosen as:

$$\begin{aligned}\boldsymbol{Q} &= \mathrm{diag}(\Theta_1^2; \Theta_2^2; \Theta_3^2; \Theta_4^2)\ \text{ and}\\ \boldsymbol{R} &= \mathrm{diag}(\Phi_1^2; \Phi_2^2; \Phi_3^2; \Phi_4^2; \Phi_5^2; \Phi_6^2; \Phi_7^2).\end{aligned} \tag{32}$$

where Θ_i and Φ_i are given as

$$\Theta_i = \zeta\left(\frac{\theta_i}{\boldsymbol{z}^2_{i\,max}}\right) and\, \Phi_i = \left(\frac{\phi_i}{\boldsymbol{e}^2_{y,i_{max}}}\right).$$

The values of the constants θ_i and ϕ_i are chosen in such a way that the state reconstruction and the measurement error convergence are sufficiently fast. The value ζ sets the relative weighting between $\boldsymbol{Q}$ and $\boldsymbol{R}$. In case of $\boldsymbol{G}_2$, both $\boldsymbol{Q} \in \mathbb{R}^{7\times7}$

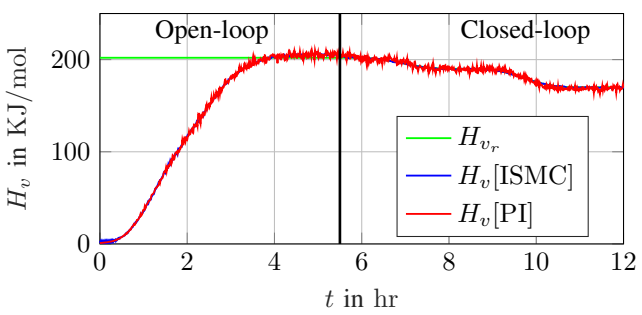

(a) Tracjectory tracking of heating value.

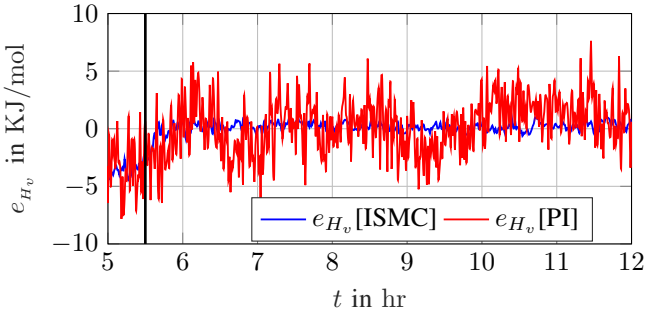

(b) Tracking error for ISMC and PI controller.

Fig. 2: Trajectory tracking and error in the heating values.

and $\boldsymbol{R} \in \mathbb{R}^{7\times7}$ are chosen to facilitate rapid convergence of $\boldsymbol{e_y}$.

Moreover, the discontinuous gains M_i in (23) need to satisfy the inequality

$$M_i > ||(\boldsymbol{A}_{21})_i \bar{\boldsymbol{e}}_z + (\bar{\boldsymbol{A}}_{22})_i + \boldsymbol{e}_y||_\infty, \tag{33}$$

where i represents the i_{th} row of a matrix.

Fig. 2 shows the trajectory tracking and the corresponding tracking error for the heating value. Therein, both the ISMC as well as the PI controller are shown. In order to quantitatively evaluate the performance of both controllers, the root-mean-square error (RMSE) given by

$$\text{RMSE} = \sqrt{\frac{1}{N}\sum_{i=1}^{N} e(i)^2}\ , e(i) = H_v(i) - H_{v_r}(i) \tag{34}$$

is computed, where N is the number of samples. The RMSE for the integral sliding mode control and the PI controller are 0.4674 KJ/mol and 2.3890 KJ/mol, respectively.

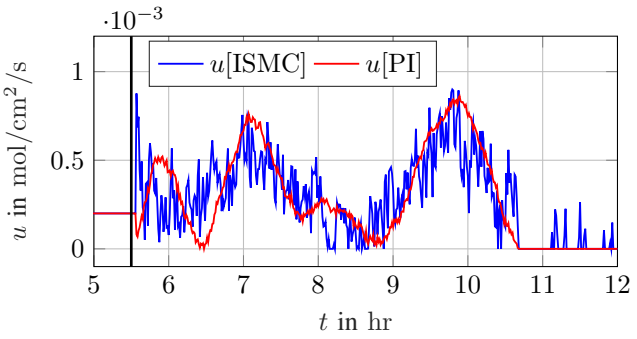

Fig. 3: Control input.

In Fig. (2b), the tracking error is shown from that time onwards when the controller is brought into operation. The control effort for the ISMC and PI control is depicted in Fig. 3. The comparison of the gas concentration–namely O_2, Tar and CH_4–available as measurements and their estimates provided by the GSMUO is depicted is Fig. 4. Here it can be clearly seen that the effects of measurement noise are filtered by the estimator. The estimated solid temperature along with

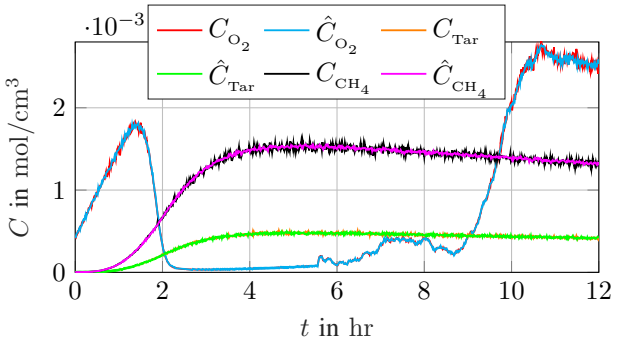

Fig. 4: Actual and estimated concentrations of gases.

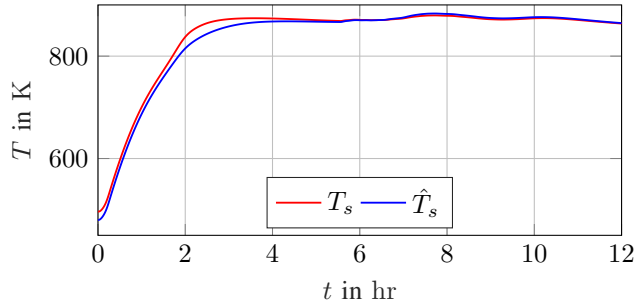

Fig. 5: Estimation of solid temperature.

the true solid temperature from the UCG plant shows a good agreement in estimation quality, see Fig. 5.

The concentration of measured and estimated gases, i.e., CO, CO_2, H_2 and N_2 are shown in Fig. 6. Herein, the GSMUO also filters out the measurement noise introduced in the UCG plant.

The densities of coal and char estimated from the GSMUO also exhibit a good estimation quality, cf. Fig. 7. The steam concentration is another important candidate for the model-based control. The actual and the estimated concentrations of steam in Fig. 8 show a good agreement.

VII. Conclusion and Future Outlook

In this paper, a gain-scheduled nonlinear control-oriented model of UCG is used to develop an ISMC for the tracking of desired heating values. To enable feedback control the

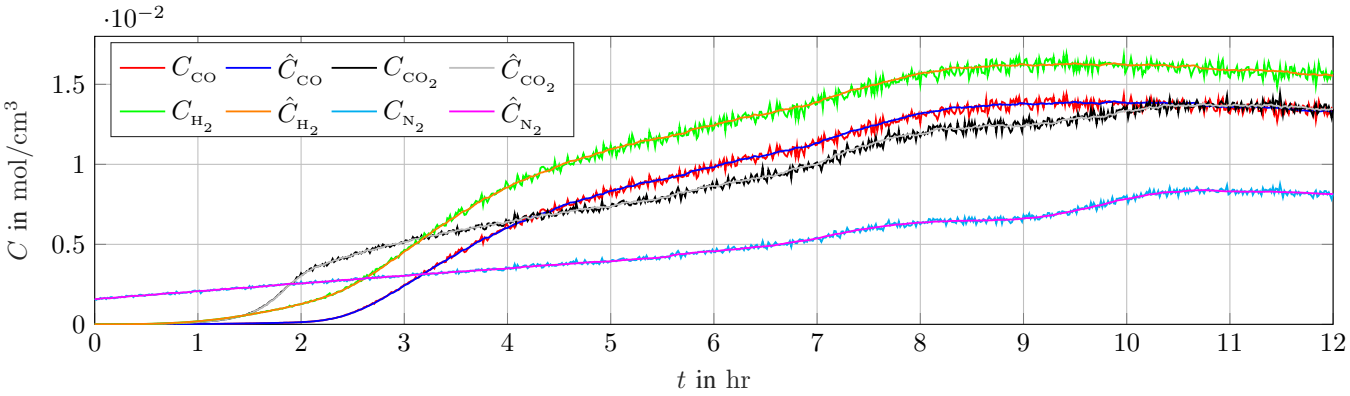

Fig. 6: Actual and estimated concentrations of product gases.

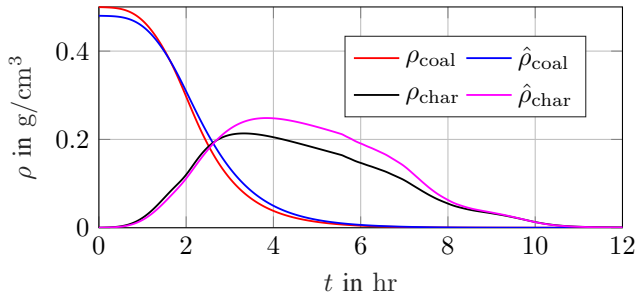

Fig. 7: Estimation of coal and char densities.

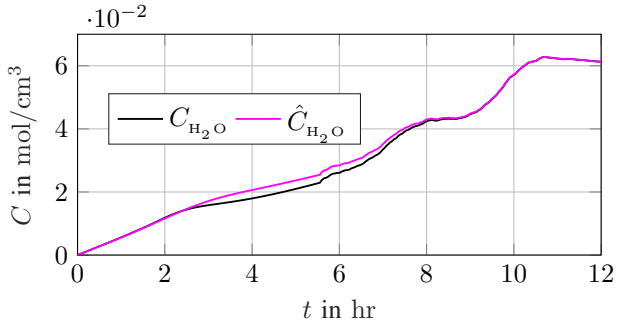

Fig. 8: True and estimated concentrations of H_2O.

unknown states of UCG plant are reconstructed using the GSMUO. For a robust state reconstruction, the gain matrices for the observer are designed using an LQR method and adapted by gain-scheduling techniques. The simulation results highlight the effectiveness of the model-based control and the GSMUO in the presence of parametric uncertainties as well as measurement noise. This research work serves as a prototype for the development of model-based control of complex infinite dimensional process models of UCG and, subsequently, for the control of field scale UCG processes.

References

[1] A. W. Bhutto, A. A. Bazmi, and G. Zahedi, "Underground coal gasification: From fundamentals to applications," *Progress in Energy and Combustion Science*, vol. 39, no. 1, pp. 189 – 214, 2013.

[2] A. Khadse, M. Qayyumi, S. Mahajani, and P. Aghalayam, "Underground coal gasification: A new clean coal utilization technique for India," *Energy*, vol. 32, no. 11, pp. 2061 – 2071, 2007.

[3] G. M. P. Perkins, *Mathematical Modelling of Underground Coal Gasification*. PhD thesis, The University of New South Wales, 2005.

[4] K. Kostúr and J. Kačúr, "The monitoring and control of underground coal gasification in laboratory conditions," *Acta Montanistica Slovaca*, vol. 13, no. 1, pp. 111–117, 2008.

[5] K. Kostur and J. Kacur, "Development of control and monitoring system of UCG by promotic," in *2011 12th International Carpathian Control Conference (ICCC)*, pp. 215 –219, may 2011.

[6] A. Arshad, A. Bhatti, R. Samar, Q. Ahmed, and E. Aamir, "Model development of ucg and calorific value maintenance via sliding mode control," in *2012 International Conference on Emerging Technologies (ICET)*, pp. 1–6, 2012.

[7] A. A. Uppal, A. I. Bhatti, E. Aamer, R. Samar, and S. A. Khan, "Optimization and control of one dimensional packed bed model of underground coal gasification," *Journal of Process Control*, vol. 35, pp. 11 – 20, 2015.

[8] A. A. Uppal, Y. M. Alsmadi, V. I. Utkin, A. I. Bhatti, and S. A. Khan, "Sliding mode control of underground coal gasification energy conversion process," *IEEE Transactions on Control Systems Technology*, vol. PP, no. 99, pp. 1–12, 2017.

[9] C. Edwards and S. Spurgeon, *Sliding Mode Control: Theory And Applications*. Series in Systems and Control, Taylor & Francis, 1998.

[10] Y. Xiong and M. Saif, "Sliding mode observer for nonlinear uncertain systems," *IEEE Transactions on Automatic Control*, vol. 46, pp. 2012–2017, Dec 2001.

[11] C. B. Thorsness and R. B. Rozsa, "Insitu coal-gasification: Model calculations and laboratory experiments," *Society of Petroleum Engineers Journal*, vol. 18, pp. 105–116, 1978.

[12] A. Winslow, "Numerical model of coal gasification in a packed bed," *Symposium (International) on Combustion*, vol. 16, no. 1, pp. 503 – 513, 1977.

[13] A. A. Uppal, A. I. Bhatti, E. Aamir, R. Samar, and S. A. Khan, "Control oriented modeling and optimization of one dimensional packed bed model of underground coal gasification," *Journal of Process Control*, vol. 24, no. 1, pp. 269–277, 2014.

[14] G. E. I. T. EUROPE, *GAS 3100 R Coal gas/Syngas 19-3U Analyser*. Gas Engineering and Instrumentation Technologies Europe, B-3380 Bunsbeek, Belgium, 2011.

[15] A. Fossard and T. Floquet, "An overview of classical sliding mode control," in *Sliding Mode Control in Engineering* (J. P. Barbot and W. Perruquetti, eds.), Control Engineering, New York, NY, USA: Marcel Dekker, Inc., 2002.

[16] M. C. M. Teixeira and S. H. Zak, "Stabilizing controller design for uncertain nonlinear systems using fuzzy models," *IEEE Transactions on Fuzzy Systems*, vol. 7, pp. 133–142, Apr 1999.

[17] S. S. Butt, R. Prabel, and H. Aschemann, "Second-order sliding mode control of an innovative engine cooling system," in *IECON 2015 - 41st Annual Conference of the IEEE Industrial Electronics Society*, pp. 002479–002484, Nov 2015.